Journal of Biomolecular Structure and Dynamics

ISSN: (Print) (Online) Journal homepage: https://www.tandfonline.com/loi/tbsd20

New tamoxifen analogs for breast cancer therapy: synthesis, aromatase inhibition and *in silico* studies

Hasan Al-Kelabi, Dunya Al-Duhaidahawi, Khattab Al-Khafaji & Najim A. Al-Masoudi

To cite this article: Hasan Al-Kelabi, Dunya Al-Duhaidahawi, Khattab Al-Khafaji & Najim A. Al-Masoudi (2023) New tamoxifen analogs for breast cancer therapy: synthesis, aromatase inhibition and *in silico* studies, Journal of Biomolecular Structure and Dynamics, 41:22, 12798-12807, DOI: 10.1080/07391102.2023.2175375

To link to this article: https://doi.org/10.1080/07391102.2023.2175375

JOURNAL OF BIOMOLECULAR STRUCTURE AND DYNAMICS
2023, VOL. 41, NO. 22, 12798–12807
https://doi.org/10.1080/07391102.2023.2175375

New tamoxifen analogs for breast cancer therapy: synthesis, aromatase inhibition and *in silico* studies

Hasan Al-Kelabi[a], Dunya Al-Duhaidahawi[b], Khattab Al-Khafaji[c] and Najim A. Al-Masoudi[d]*

[a]Pharmacy Department, AL-Najaf Health Directorate, Ministry of Health, Najaf, Iraq; [b]Department of Pharmacognosy, College of Pharmacy, University of Kufa Al-Najaf, Kufa, Iraq; [c]Pharmacy Department, Al-Maarif University College, Anbar, Iraq; [d]Department of Chemistry, College of Science, University of Basrah, Basrah, Iraq

Communicated by Ramaswamy H. Sarma

ABSTRACT

A new class of tamoxifen analogues, using McMurry reaction conditions, is described. The scheme involved the conversion of ketoprofen (**6**) into amide derivatives **7** and **8**, by coupling with N^1,N^1-substituted propan-1,3-diamine derivatives in the presence DIC and HOB. Treatment of **7** and **8** with various ketones under McMurry reaction conditions afforded the tamoxifen analogues **9–16**. All the analogues were screened *in vitro* for their aromatase inhibitory and antiproliferative activity against MCF-7 breast cancer cells. Compounds **10, 11** and **12** showed a potent activity against MCF-7 cell lines breast cancer with IC_{50} values of 0.070, 0.042 and 0.077 μM of selectivity index (SI) 3.0, 2.5 and 2.6, respectively. Further, **12** exhibited potent activity against estrogen receptor (14.7 ± 2.4 nM), while compound **10** was the most active analogues against aromatase with IC50 of (0.070 nM). Furthermore, all new compounds were docked into human placental aromatase enzyme and estrogen receptor and showed very good correlations with experimental IC50. Therefore, we can consider these designed compounds as starting scaffold to design an efficient drug against estrogen receptor and aromatase.

ARTICLE HISTORY
Received 5 August 2022
Accepted 7 January 2023

KEYWORDS
Aromatase inhibitors; breast cancer; estrogen receptor (ER+); ketoprofen; molecular modelling study; tamoxifen analogues

Introduction

Breast cancer is the second most common cancer in the world and one of principal causes of death in human (Bray et al., 2018; Ferlay et al. 2015). Since almost 80% of breast cancer cases are hormone-dependent, estradiol acting via the estrogen receptor (ER) plays a major role in the growth and development of (ER+) breast cancer. Estrogen receptor (ER) positive tumors are present in 60% of premenopausal and 75% of postmenopausal cancer patients and response to hormone replacement (antiestrogen treatment; Jordan & Brodie, 2007). Inhibition of estradiol by aromatase inhibitors is the most successful treatment of breast cancer. Aromatase inhibitors like tamoxifen **1** (Double et al., 2001; Fisher et al., 2005; Srikanth et al., 1997), anastrozole **2** (Bonneterre et al., 2001; Ellis et al., 2015), letrozole **3** (Bonneterre et al., 2001) and exemestane **4** (Brueggemeier et al., 2005; Coombes et al. 2007) are considered as the most effective drugs for treatment of positive α- and β-estrogen receptors (ER) breast cancer, the structures of some anti-breast cancer drugs as aromatase inhibitors illustrated in Figure 1 (Choueiri et al., 2004). Tamoxifen has been widely used for over 30 years to treat ER-positive women with breast cancer (Cuzick et al., 2015; Davies et al., 2013) in a period of 5 years. It is metabolized into the more active 4-hydroxytamoxifen by CYP2D6 enzyme (Cronin-Fenton et al., 2014). Norendoxifen **5** (Lu et al., 2012; Lv et al., 2013) is another non-steriodal potent aromatase inhibitor with IC_{50} 90 nM, and its action mode showed that it targeted CYP450 aromatase. Additionally, exploration of the endocrine pharmacology of tamoxifen and related nonsteroidal antiestrogen (e.g., keoxifene now known as raloxifene) resulted in the laboratory recognition of selective ER modulation and the translation of the concept to use raloxifene for the prevention of osteoporosis and breast cancer. Other drugs like formestane (Carlini et al., 2001), and fadrozole (Browne et al., 1991) are considered as potent aromatase inhibitors. Several laboratories have reported the synthesis of various analogues of tamoxifen with their aromatase inhibitory activity in comparison itself, meanwhile some of these analogues exhibited significant activity against breast cancer of ER+ (Abdellatif et al., 2013; Carpenter et al., 2017; Elghazawy et al., 2016; Ohta et al., 2019; Olier-Reuchet et al., 1998; Sharma et al., 2018). Much more recently, Banday et al. (2021) have synthesized new series of pregnenolone of functionally diverse D-ring pregnenolone pyrazoles. However, aromatase inhibitors can cause reduced bone density, considerable musculoskeletal pain and cardiovascular and venous thromboembolism events (Gaillard & Stearns, 2011; Hyder et al., 2021).

The work here is focused on designing and synthesis of new tamoxifen analogues as selective estrogen receptor

CONTACT Dunya Al-Duhaidahawi dunyal.mohammed@uokufa.edu.iq Department of Pharmacognosy, College of Pharmacy, University of Kufa Al-Najaf, Kufa, 31001, Iraq

Supplemental data for this article can be accessed online at https://doi.org/10.1080/07391102.2023.2175375.

*Present: Najim A. Al-Masoudi 78464 Konstanz, Germany.

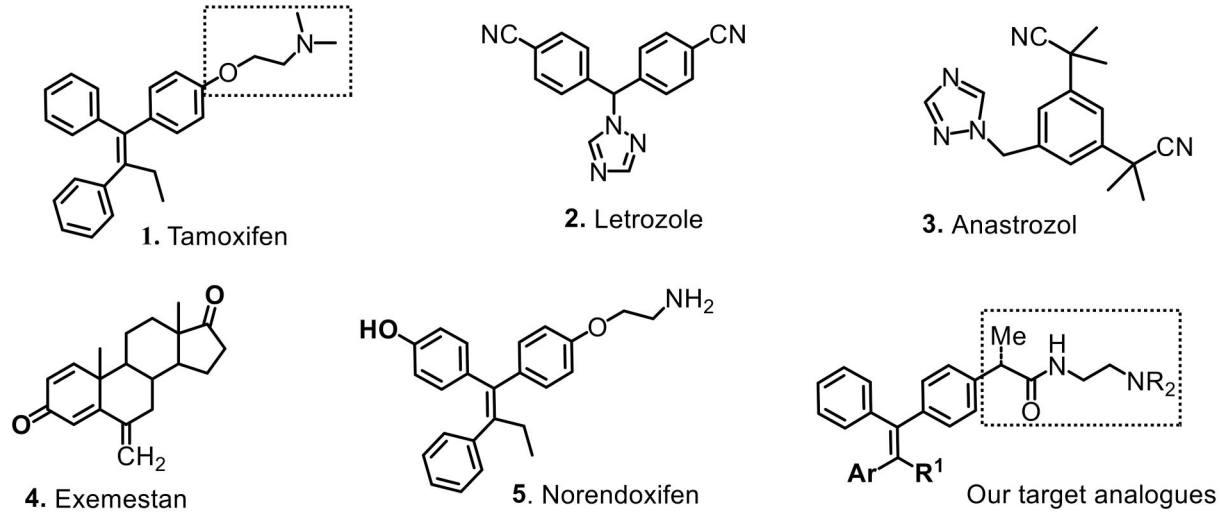

Figure 1. Some anti-breast cancer drugs as aromatase inhibitors (Choueiri et al., 2004).

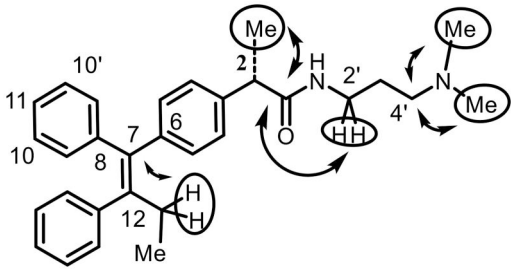

Figure 2. $J_{C,H}$ correlations in the NMR HMBC correlations of (**13**).

modulators (SERMs) against MCF-7 breast cancer cell lines by inhibition of aromatase enzyme and studying the binding of these new analogues with the estrogen receptors (ER), and counteract β-estradiol effect. Moreover, molecular docking is attended to shed light on how can these series of synthesized compounds interacted with targeted proteins.

Results and discussion

Chemical synthesis

In the present work, the non-steriodal anti-inflammatory drug ketoprofen **6** has been selected as a starting material for the design and synthesis of new tamoxifen analogs. Thus, treatment of **6** with N^1,N^1-dimethyl-1,3-propandiamine and 3-(pyrrolidine-1-yl)propan-1-amine in the presence of DIC and HOBt afforded the amide derivatives **6** and **7** in 71 and 75% yield, respectively. Treatment of **6** and **7** with various ketones (e.g., propiophenone, 1-(4-fluorophenyl)pentane-1-one, (4-Fluorophenyl)(4-hydroxyphenyl)methanone, and 1-(3,5-difluorophenyl)propan-1-one) under McMurry conditions reaction in the presence $TiCl_4$/Zn afforded the required tamoxifen analogues **9–16**.

The structures of **9–16** were confirmed by their IR, ^{1}H and ^{13}C NMR and mass spectra. The aromatic and aliphatic protons showed a similar pattern. In the ^{1}H NMR spectra of **9–16**, H-2 appeared as a quartet in the range δ 3.78–3.60 ppm (for both *R,S* isomers), while methylene protons CH_2-2′ resonated as multiplet in the range δ 3.40–3.11 ppm. CH_2-3′ protons appeared as a multiplet in the range $\delta = 1.76$–1.72 ppm, while NCH_2-1′ protons resonated as multiplet in the range δ 2.15–2.47 ppm. The methyl group at C-2 was resonated as a doublet in the range δ 1.43–1.34 ppm. The pyrrolidine protons of compounds **13–16** appeared in the regions δ 2.59–2.55 and 1.90–1.73 ppm. The aromatic and other aliphatic protons were fully analyzed (*c.f.* Experimental section). In the ^{13}C NMR spectra of **9–16**, the carbonyl carbon atoms of amide moiety $HNC_1{=}O$ resonated in the ranges δ 173.9–173.7 ppm, while the resonances in the range δ 45.4–39.33 ppm assigned to C-2 carbon atom. C-2′ and C-3′ of the propylamide group were appeared in the regions δ 42.9–36.3 and 31.2–26.3 ppm, respectively, whereas C-4′ of the same group of compounds **9–12** appeared in the region δ 61.2–57.6 ppm. However, C-4′ of compounds **13–16** resonated in the regions δ 40.0–38.0 ppm. The pyrrolidine carbon atoms C-2 + C-5 and C3 + C-4 appeared in the regions δ 54.9–52.7 and 24.9–23.0 ppm, respectively. C-F carbon atom resonated as a doublet in the region δ 166.6–162.7 ppm (JC, F ∼ 185 ppm). The other aromatic and aliphatic substituents carbon atoms were fully analyzed (*c.f.* "Experimental" section).

Compound **13** was selected for further NMR experiment. In the gradient-selected HMBC spectrum (Willker et al. 1998) NMR spectrum of **9** showed two $^3J_{C;H}$ heteronuclear correlations: CH_2-2′ at δ_H 3.25 ppm as well as δ_H C2-Me at 3.78 ppm to the carbonyl carbon atom ($NHC1{=}O$) at δ_C 173.9 ppm, Additional two $^3J_{C;H}$ correlations were observed: both NMe_2 at δ_H 1.98 ppm correlated to C-4′ of the propyl side chain at δ_H 58.6 ppm. Moreover, a $^3J_{C;H}$ correlation between methylene protons of ethyl group at δ_H 2.20 ppm and olefinic carbon atom C-7 at δ_H 143.1 ppm was observed (Figure 2).

Biological activity evaluation

Aromatase inhibitory activity

All compounds were tested for their inhibition of aromatase activity, following Stresser method (2000) and modified by Prachayasittikul et al. (2014), using tamoxifen as a reference drug. The results are summarized in Table 1. Among all tested compounds, only **10** and **14** exhibited aromatase

Table 1. Inhibition of the human aromatase enzyme by new tamoxifen analogues.

Compd.	IC_{50} (nM)	Ki (nM)	Compd.	IC_{50} (nM)	cKi (nM)
9	58.3 ± 3.8	48.0 ± 0.9	**14**	14.7 ± 0.9	27.5 ± 2.7
10	28.9 ± 1.4	38.6 ± 5.2	**15**	46.4 ± 1.9	56.8 ± 2.1
11	101.7 ± 1.4	65.0 ± 3.2	**16**	63.6 ± 1.7	106 ± 3.7
12	109.4 ± 2.8	75.0 ± 3.2	TAM	38.1 ± 2.9	31 ± 1.2
13	36.6 ± 0.8	78.4 ± 1.2			

TAM: tamoxifen was used as a reference standard.
Ki: is dissociation constant describing the binding affinity between the inhibitor and the enzyme in nM.

Table 2. Tamoxifen and prepared analogues (H1–H8) estrogen receptor binding affinities.

Code	ER-α (EC50, nM)	ER-β (EC50, nM)
9	36.6 ± 3.8	48.4 ± 1.2
10	34.7 ± 2.9	48 ± 2.7
11	26.4 ± 1.9	56.8 ± 4.1
12	14.7 ± 2.4	27.5 ± 2.7
13	42.5 ± 2.6	51.4 ± 5.3
14	28.8 ± 4.3	35.8 ± 4.8
15	51.8 ± 2.4	49.7 ± 7.2
16	37 ± 6.7	57 ± 1.6
Tamoxifen	26 ± 1.2	15.3 ± 2.2

inhibitory effect in a dose-dependent manner, particularly more potent than the positive control, tamoxifen with IC_{50} of 28.9 ± 1.4 and 14.7 ± 0.9 nM with Ki values of 38.6 ± 5.2 and 27.5 ± 2.7, respectively.

The SAR study suggested that the introduction of moderate hydrophilic substituent such as *N*-propyl amide substituent, in addition to the *N*-dimethylamino group, would enhance the aromatase inhibitory activity in comparison to the ether group as in tamoxifen (Table 2). However, introduction of 4-OH-Ph moiety instead of olefinic alkyl group did not show any effect on the inhibitory activity.

Estrogen receptors affinity

Anti-breast cancer activity

The newly synthesized compounds **9–16** were evaluated for their *in vitro* antiproliferative potential against MCF-7 and Vero cell lines by MTT assay (Mosmann, 1983), using tamoxifen, paclitaxel and 5-fluorouracil as reference standards. The 50% inhibitory concentration (IC_{50}, nM) values were determined for these compounds, and the results are summarized in Table 3. Notably, all the screened analogues showed antiprolferative activity against MCF-7 cell lines; however, compounds **10**, **11** and **12** exhibited significant antiproliferative activity more than the reference drugs against MCF-7 cell lines with SI values of 3.0, 2.5 and 2.6, respectively compared to the reference drugs: tamoxifen, paclitaxel and 5-fluorouracil (SI = 0.8, 1.5 and 2.0, respectively). However, compound **13** having pyrrolidine residue exhibited a higher selectivity index than other compounds of the series (SI = 4), indicated that 13 is less toxic than the others against the Vero normal cells.

Molecular docking study

A total of 8 compounds tamoxifen series were docked into the active site of estrogen receptor and aromatase and

Table 3. Anti-breast cancer cell activity (IC_{50}) and SI values of the new tamoxifen analogues.

Compd.	MCF-7 IC_{50} (μM)	Vero IC_{50} (μM)	SI*	Compd.	MCF-7 IC_{50} (μM)	Vero IC_{50} (μM)	SI*
9	0.100	0.309	3.1	**15**	0.309	0.265	2.6
10	0.070	0.207	3.0	**16**	0.207	0.136	1.3
11	0.042	0.104	2.5	TAM	0.104	0.330	0.8
12	0.077	0.197	2.6	PAC	0.197	0.030	1.5
13	0.140	0.566	4.0	5-FU	0.566	1.085	2.0
14	0.104	0.301	2.9				

TAM: tamoxifen, PAC: paclitaxel, 5-FU: 5-fluorouracil.
SI = IC_{50} (Vero cells)/IC_{50} (MCF-7 cells). *= compound with positive selectivity index.

presented in Table 4. The correlation between docking score of 8 compounds and the IC50 against estrogen receptor was R^2 = 0.7544 (Figure 3A), whereas the good correlation is observed also between docking score of 8 compounds and the IC50 against aromatase (R^2 = 0.79) (Figure 3B). The experimentally top active compound against estrogen receptor was 12 with docking score −12.9490 kcal/mol ranked as top potent against estrogen receptor, which exhibited binding affinity higher than TAM (−11.5684 kcal/mol). Further, the binding mode is represented in Figure 4. From Figure 4 we can see that **12** interacted with estrogen receptor via two hydrogen bonds with Asp351 besides 1 attractive interaction. And nine hydrophobic interactions with Leu525, Leu384, Met388, Leu391, Leu346, Leu387 and Ala350. Furthermore, top active compound against aromatase was **14** with docking score −10.0168 kcal/mol, which also better than docking score of TAM against aromatase −7.8631 kcal/mol. The **10**-aromatase interaction is depicted in Figure 5. Where **10** formed seven hydrogen bonds with Arg375, Asp309, Gly346, Ser478, Arg435 and Cys437. Moreover, **10** interacted with aromatase via eight hydrophobic interactions and four electrostatic interactions, as presented in Figure 5.

ADME prediction

Compounds **9–16** have been studied for their pharmacokinetic profile ADME (absorption, distribution, metabolism, and excretion), as well as other parameters, such as BBB penetration, Pg. affinity, and bioavailability by using SwissADME tool (Daina et al., 2017). It is used to discover the safe and most usually reliable candidate drug in order to remove those molecules with poor ADME properties that are most prone to failure in later phases of drug discovery. In this study, we have calculated nRB, nHBA, nHBD, TPSA (A), BS, GI absorption, BBB, Pgp, iLOGP and percentage human oral absorption and Lipinski's rule of five using QikProp. The results are displayed in Table 5. Figure 6 demonstrated the correlation between the percentage growth inhibition of compound **14**, as example, and the Log concentrations, meanwhile the rest of Figures 5–24 are presented in Supplementary material.

Experimental

General

Melting points were determined on a Mel-Temp device melting point apparatus and are uncorrected. The IR spectra

were recorded, on FT-IR Spectrophotometer (Thermo Nicolet Corp., USA), using KBr discs. ^{1}H and ^{13}C NMR spectra were recorded on Bruker Avance (400 MHz) (^{1}H) and 125.65 MHz (^{13}C) spectrometers, using DMSOd_6 solvent containing tetramethyl silane as an internal standard (chemical shifts in δ in ppm). FAB mass spectra were recorded on MAT 8200 mass spectrometer (Finnegan MAT, USA) using 3-nitrophenol, sodium iodide or glycerol as matrix. The reactions were monitored by thin layer chromatography (eluent:hexane-EtOAc 4:1), and the spots were visualized by iodine and U.V.

General procedure for the synthesis of amide derivatives of ketoprofen via McMurry cross-coupling reaction (7 and 8)

Coupling is done by the conventional solution method. To a stirred solution of ketoprofen (**6**) (254 mg, 1.00 mmol) in (10 mL) DMF, HOBt (243 mg, 1.8 mmol) was added followed by addition of DIC (126 mg, 1.00 mmol) and stirring continue for 45 minutes. propyl-1,3-diamine derivative (1.1 mmol) was added to the reaction mixture. After stirring for 72 h at room temperature, the mixture was evaporated to dryness and the residue was portioned between ethyl acetate (20 mL) and water (20 mL). The filtrate was washed with 0.1 N HCl (2 × 5 mL), then with saturated NaCl solution (10 mL) and finally with water (10 mL). The organic layer was dried ($MgSO_4$), filtered and the filtrate was evaporated to dryness. The syrupy crude product was purified on a short SiO_2 column using a mixture of (CH_2Cl_2:MeOH:methanolic NH_3) (9:0.5:0.5) as eluent to give a pure product.

2-(4-Benzoylphenyl)-N-(3-dimethylamino)propyl)propenamide (7)

From N^1,N^1-(dimethyl amino)propan-1-amine (139 mg). Yield: 240 mg yield (71%) as a faint yellow oil; IR (neat, cm^{-1}): 3348 (NH), 3095 (Ar*CH*), 2984 (CH_3), 1676 (C = O_{amide}), 1662 (C = O), 1572 (C = C). ^{1}H NMR (DMSO-d_6): δ = 7.78–7.51 (m, 9H, ArH), 6.87 (br s., 1H, NH), 3.68 (qt, 2H, $J_{H2,Me}$ = 6.0, 1.0 Hz, H-2 (*R,S*-isomers), 3.14 (m, 2H, $NHCH_2'$), 2.48 (m, 2H, Me_2NCH_2-4′), 1.98 (2xs, 6H, NMe_2), 1.74 (m, 2H, CH_2-3′), 1.34 (d, J = 6.0 Hz, 6H, C_2-Me (*R,S*-isomers). MS (FAB) (*m/z*): $C_{21}H_{26}N_2O_2$ 339 $[M+H]^+$.

2-(4-Benzoylphenyl)-N-(3-pyrrolidin-1-yl)propyl)propenamide (8)

From 1-amino-2-(pyrollidin-1yl)propane (141 mg). Yield: 273 mg (75%) as a dark yellow oil; IR (neat, cm^{-1}): 3348 (NH), 3095 (Ar*CH*), 2970, 2936 (aliph.CH_3), 1620 (C = O_{amide}), 1572 (C = C). ^{1}H NMR (DMSO-d_6) δ = 7.84–7.50 (m, 9H, ArH), 6.89 (br s., 1H, NH), 3.68 (qt, 2H, $J_{H2,Me}$ = 6.0, 1.0 Hz, H-2 (R,S isomers), 3.16 (m, 2H, $NHCH_2'$), 2.62 (m, 4H, 2x$CH_{2pyrrol.}$), 2.55 (m, 2H, Me_2NCH_2-4′), 1.85 (m, 4H, 2x$CH_{2pyrrol.}$), 1.76 (m, 2H, CH_2-3′), 1.34 (d, J = 6.0 Hz, 3H, C_2-Me (R,S isomers). ^{13}C NMR (DMSO-d_6): δ = 194.0 (C_7=O), 173.2 (NHC_1=O), 141.2 ($C_{arom.}$-3), 140.0 ($C_{arom.}$-6 + $C_{arom.}$-8), 132,9, 1323, 131.8, 130.4, 128.8 ($C_{arom.}$), 58.6 ($C^2_{pyrrol.}$+$C^5_{pyrrol.}$), 45.4 (C_2-*Me*), 40.4 (C-4′), 31.3 (C-3′), 26.7 ($C3_{pyrrol.}$+$C4_{pyrrol.}$), 18.9 (Me). MS (FAB) (*m/z*): $C_{23}H_{28}N_2O_2$ 365 $[M+H]^+$.

General procedure for the synthesis of tamoxifen analogues (9–16) under McMurry reaction conditions

Zinc powder (595 g, 9.15 mmol) was suspended in dry THF (25 mL) and chilled to °C under argon, followed by addition of $TiCl_4$ (380 mg, 1.94 mmol). The mixture was then heated to room temperature and heating under reflux for 2 h. After cooling, ketoprofen amide (**6**) (200 mg, 1.00 mmol) and various ketones (2.90 mmol) in dry THF (100 mL) were added with stirring at 0 °C. The mixture was then heated under reflux in the dark for 3 h. After cooling, zinc dust was filtered and THF was evaporated to dryness. The residue was dissolved in dil. NH_4Cl solution (100 mL) and extracted with ethyl acetate (2 × 50 mL). The organic layers were combined, dried (Na_2SO_4), filtered and evaporated to dryness. The crude product was purified on SiO_2 column (50 g) and eluted with hexane-ethyl acetate 2:1 to give the pure desired product.

N-(3-(dimethylamino)propyl)-2-(3-(1,2-diphenylbut-1-en-1-yl)phenyl)propenamide (9)

From propiophenone (389 mg). Yield: 299 mg (68%) as a faint yellow oil; IR (cm^{-1}): 33378 (NH), 3116 (Ar*CH*), 2971, 2933 (Me), 1666 (C = O_{amide}), 1622 (ArC = C), 1572 (C = C). ^{1}H NMR (DMSO-d_6): δ = 7.57–7.03 (m, 14H, ArH), 6.88 (br s., 1H, NH), 3.78 (q, 1H, $J_{H2,Me}$ = 5.9, H-2 (R,S isomers), 3.25 (m, 2H, $NHCH_2$-2′), 2.47 (m, 2H, Me_2NCH_2-4′), 2.20 (q, 2H, J = 7.3 Hz, CH_2CH_3), 1.98 (2xs, 6H, NMe_2), 1.74 (m, 2H, CH_2-3′), 1.34 (d, J = 6.0 Hz, 6H, C_2-Me (R,S isomers)), 0.94 (t, 3H, J = 7.3 Hz, CH_2CH_3). ^{13}C NMR (DMSO-d_6): δ = 173.9 (NHC_1=O), 143.1 ($C_{arom.}$-8 + $C_{arom.}$-13 + C_{olefin}-7), 137.4 ($C_{arom.}$-6), 134.0 ($C_{arom.}$-3), 132,1, 132.3, 131.1, 130.1, 129.2, 129.1, 128.8, 128.7 ($C_{arom.}$+C_{olefin}-12), 58.6 (Me_2NCH_2-4′),), 45.4 (NMe_2), 42.9 (C_2-Me + $NHCH_2$-2′), 31.2 ($Me_2NCH_2CH_2$-3′),), 24.8 (CH_2CH_3), 14.9 (Me), 14.1 (CH_2CH_3). MS (FAB) (*m/z*): $C_{30}H_{36}N_2O$ 441 $[M+H]^+$.

N-(3-(Dimethylamino)propyl)-2-(3-(2-(4-fluorophenyl)-1-phenylhex-1-en-1-yl)phenyl)propanamide (10)

From 1-(4-fluorophenyl)pentane-1-one (522 mg). Yield: 296 mg (61%) as a brown solid; m.p. 263–265 °C; IR (KBr, cm^{-1}): 3341 (NH), 3061 (Ar*CH*), 2978, 2870 (CH_3), 1657 (C = O_{amide}), 1620 (C = C), 1573 (C = C). ^{1}H NMR (DMSO-d_6): δ = 8.20 (NH), 7.96 (s, 5H, ArH), 7.78–7.67 (m, 6H, ArH), 7.67–7.54 (m, 2H, ArH), 3.68 (q, 1H, $J_{H2,Me}$ = 5.9 Hz, H-2 (R,S isomers)), 3.38 (m, 2H, $NHCH_2$-2′), 3.05 (m, 2H, NMe_2CH_2-4′), 1.98 (m, 8H, NMe_2+$BuCH_2$-1), 1.76 (m, 2H, CH_2-3′), 1.38 (m, 7H, $BuCH_2$-2 + $BuCH_2$-3 + C_2-Me (R,S isomers), 0.90 (t, 3H, J = 5.3 Hz, $BuCH_3$). ^{13}C NMR (DMSO-d_6): δ = 173.8 (NHC_1=O), 166.6 (d, $J_{C,F}$ = 184 Hz, C-F), 143.0 ($C_{arom.}$-8), 137.3 ($C_{arom.}$-6), 133.2 ($C_{arom.}$-3 + $C_{arom.}$-13), 132.0, 131.2, 129.0, 128.7, 127.8, 125.0 ($C_{arom.}$+C_7=C_{12}), 116.2 ($C^{15}{}_{arom.}$+$C^{15'}{}_{arom.}$), 61.1 (Me_2NCH_2-4′), 42.8 (NMe_2), 42.7 (C_2-Me), 38.6 (NHC-2′), 34.8 (Bu*C-2*), 31.2 (Bu*C-1*), 26.3 (C-3′), 22.2 (Bu*C-3*), 14.3 (Bu*Me*+C_2-*Me*). MS (FAB) (*m/z*): $C_{32}H_{39}FN_2O$ 485/487 $[M+H]^+$.

Table 4. Molecular docking analysis: two proteins (ER-α and aromatase) docked against eight active compounds and their properties.

Protein	Ligand	S-Score MOE (Kcal/Mol)	RMSD (Å)	Conserved residues	Average bond distance (Å)
ER-α	9	−11.3571	2.2924	Leu346; The347, Ala350, Asp351, Trp383, Met522, Leu525, Val533, Pro535, Leu536	2.82
	10	−12.0837	4.2576	Leu346;**The347;Ala350;Asp351;**Trp383;Leu387Leu391;**Leu525;** Cys530;Val533;Val534;Leu539	2.65
	11	−12.5564	4.4738	**Thr347;Ala350;Asp351;**Trp383;**Leu525;**Val533;Val534	3.03
	12	−12.9490	1.2918	Leu346;**Thr347;**Leu349;**Ala350;Asp351;**Glu353,Trp383;Leu384; Leu391;Arg394;Phe404;**Leu525**,Cys530;Val533	1.69
	13	−9.7477	5.0319	Leu346;**Thr347;Ala350;Asp351**;Glu380;Trp383;Leu384;Leu387; Leu391;Met522;**Leu525;**Tyr526;Val534;Leu536	2.83
	14	−12.6202	4.7386	Leu346;**Thr347;Ala350;Asp351**;Trp383;Leu384,**Leu525**;Met528; Lys529;Cys530;Lys531;Val533	2.64
	15	−9.2531	2.4818	Met343;Leu346;**Thr347**;**Ala350**;**Asp351**;Leu387,**Leu525**;Met528;Cys530	3.08
	16	−9.8587	3.8008	Leu346;**Thr347;Ala350;Asp351**;Leu384;**Leu525**,Cys530;Val533	3.66
	TAM	−11.5684	1.6881	Leu346;Thr347;Ala350;Asp351;Glu380;Trp383;Leu384;**Leu387**; Leu391;Met522;Leu525;Tyr526;Val534;Leu536	4.57
Aromatase	9	−7.5178	1.3952	**Arg115**;Ile132;Ile133;Arg145;Leu152;Trp224;Ala306;Ala307;Met311; **Val370**;Leu372;Val373;Met374,Phe430;Cys437;Ala438;**Gly439**; Ile442;**Ala443**,Met446	1.96
	10	−9.4989	2.6217	**Arg115**;Ile133;Phe134;Leu152;Phe203;Phe221;Trp224;Ala306;Ala307; Thr310;Met311;**Val370**;Leu372,Val373;Met374;Phe430;Cys437; **Gly439**;Ile442;**Ala443**;Met446;Leu477	2.37
	11	−7.3758	1.6567	**Arg115**;Ile133;Phe134;Leu152;Phe203;Phe221;Met303;Ala306;Ala307; Asp309;Thr310;Met311;**Val370**;Leu372;Val373;Met374;Phe430; Lys437;**Gly439;Ala443**;Met446;Ser478	3.85
	12	−6.4318	1.0134	**Arg115**;Ile132;Ile133;Arg145;Leu152;Phe221;Trp224Ala306;Ala307; Asp309;Thr310;**Val370**;Leu372;Val373;Met374;Arg435;Gly436; Cys437;Ala438;**Gly439Ala443**;Ser478	3.69
	13	−8.8957	1.3717	**Arg115**;Ile132;Ile133;Leu152;Trp224;Ala307;**Val370**Leu372;Val373; Met374;Phe430;Cys437;Ala438;**Gly439**;Ile442;**Ala443**;Met446	2.19
	14	−10.0168	1.8066	**Arg115**; Phe134; Leu152; Trp224; Ala306; Ala307 Thr310; Met311; Ser314; Val369; **Val370**;Val373,Met374;Pro429;Phe430;Arg435; **Gly439,Ala443;**Met446	2.08
	15	−8.2793	1.1891	**Arg115**;Ile133;Phe134;Trp224;Ala306;Thr310,**Val370**;Val373;Phe430; Gly431;Cys437;Ala438,**Gly439**;**Ala443**;Leu477	1.93
	16	−7.7888	1.8654	**Arg115**;Ile132;Phe134;Phe221;Trp224;Ala306,Thr310;Met311;**Val370**; Pro429;Arg435;Gly436,Cys437;Ala438;**Gly439**;**Ala443**;Met446;Leu477	2.06
	TAM	−7.8631	1.74289	Arg115;Ile132;Phe134;Phe221;Trp224;**Ala306**,Thr310;**Met311**;Val370; Pro429;Arg435;Gly436,**Cys437**;Ala438;**Gly439**;Ala443;Met446;Leu477	3.378

Bold values signifies the most conserved active binding residues among binding residues of estrogen receptor alpha protein and aromatase. All eight active compounds bound to these conserved residues among other non-conserved residues.

N-(3-(dimethylamino)propyl)-2-(3-(2-(4-fluorophenyl)-2-(4-hydroxyphenyl)-1-phenylvinyl)phenyl) propenamide (11)

From (4-Fluorophenyl)(4-hydroxyphenyl)methanone (626 mg). Yield: 370 mg (71%) as a brown oil; IR (neat, cm^{-1}): 3338 (NH), 3057(Ar*CH*), 2972, 2887 ($CH_{aliph.}$), 1657 ($C=O_{amide}$), 1560 (C = C). ^{1}H NMR (DMSO-d_6): $\delta = 10.5$ (OH), 8.21 (NH), 7.90 (s, 3H, ArH), 7.76 (ddd, $J = 10.0$, 6.2, 3.1 Hz, 2H, ArH), 7.73–7.62 (m, 2H, ArH), 7.64-7.49 (m, 1H, ArH), 7.37 (t, 2H, $J = 8.9$ Hz, ArH), 6.96-6.88 (m, 4H, ArH), 3.60 (q, 1H, $J_{H2,Me}$ = 6.0 Hz, H-2 (R,S isomers)), 3.35 (m, 2H, $NHCH_2$-2′), 2.90 (m, 2H, Me_2NCH_2-4′), 1.94 (m, 8H, NMe_2), 1.72 (m, 2H, CH_2-3′), 1.43 (d, $J = 6.0$ Hz, C_2-Me (R,S isomers)). ^{13}C NMR (DMSO-d_6): $\delta = 173.9$ (NHC_1=O), 165.8 (d, $J_{C,F}$ = 185 Hz, C-F), 163.3 (C-OH), 137.4 ($C_{arom.}$-8 + C_7=C_{12}), 137.3 ($C_{arom.}$-6), 135.0 ($C_{arom.}$-13), 134.9 ($C_{arom.}$-3 + $C_{arom.}$-5 + $C_{arom.}$-5′), 130.0, 129.0, 128.7, 128.2, 116.2, 115.1 ($C_{arom.}$), 61.2 (Me_2NCH_2-4′), 45.4 (NMe_2), 41.2 (NHC-3′+C_2-Me), 36.3 (C-2′), 31.1 (C-3′), 14.9 (Me). MS (FAB) *(m/z)*: $C_{34}H_{35}FN_2O2$ 521/523 $[M+H]^+$.

2-(3-(2-(3,5-Difluorophenyl)-1-phenylbut-1-en-1-yl)phenyl)-N-(3-(dimethylamino)propyl)propenamide (12)

From 1-(3,5-difluorophenyl)propan-1-one (493 mg). Yield: 319 mg (67%). as a light brown oil; IR (neat, cm^{-1}): 3418 (NH), 3100 (Ar*CH*), 2970, 2936 ($CH_{aliph.}$), 1655 ($C=O_{amide}$), 1562 (C = C). ^{1}H NMR (DMSO-d_6): $\delta = 8.22$ (s, 1H, NH), 7.92 (s, 3H, ArH), 7.71 (m, 2H, ArH),7.50 (m, 4H, ArH), 6.90–6.64 (m, 3H, ArH), 3.73 (q, 1H, $J_{H2,Me}$ = 6.0 Hz, H-2 (R,S isomers), 3.37 (m, 2H, $NHCH_2$-2′), 3.15 (m, 2H, Me_2NCH_2-4′), 2.25 (q, 2H, $J = 5.2$ Hz, CH_2CH_3), 1.97 (s, 6H, NMe_2), 1.75 (m, 2H, CH_2-3′), 1.37 (d, $J = 6.0$ Hz, 6H, C_2-Me (R,S isomers)), 1.18 (t, 3H, $J = 5.3$ Hz, CH_2CH_3). ^{13}C NMR (DMSO-d_6): $\delta = 173.8$ (NHC_1=O), 162.7 (d, $J_{C,F}$ = 187 Hz, CF), 143.1 ($C_{arom.}$-8 + $C_{arom.}$-13), 137.4 ($C_{arom.}$-6), 136.3 ($C_{arom.}$-3 + $C_{arom.}$-5 + $C_{arom.}$-5′), 130.1 129.1, 128.8 128.7 128.2, 110.1, 105.2 ($C_{arom.}$+C_7=C_{12}), 57.6 (Me_2NCH_2-4′), 45.4 (NMe_2), 42.8 (C_2-Me), 36.8 (NHC-2′), 31.2 (CH_2CH_3+CH_2-CH-3′), 14.8 (CH_2CH_3+C_2-*Me*). MS (FAB) *(m/z)*: $C_{30}H_{34}F_2N_2O$ 475/477 $[M+H]^+$.

2-(3-(1,2-Diphenylbut-1-en-1-yl)phenyl)-N-(3-(pyrrolidin-1-yl)propyl)propenamide (13)

From propiophenone (389 mg). Yield: 298 mg (64%) as a pale-yellow oil; IR (neat, cm^{-1}): 3340 (NH), 3063 (ArCH), 2974, 2880 (CH_3), 1622 ($C=O_{amide}$), 1574 (C = C). ^{1}H NMR (DMSO-d_6): $\delta = 9.29$ (s, 1H, NH(, 8.21–7.20 (m, 14H, ArH), 3.71 (q, 1H, $J_{H2,Me}$ = 6.0, 1.0 Hz, H-2 (R,S isomers)), 3.11 (m, 2H, $NHCH_2$-2′), 2.56 (m, 6H, CH_2-4′+2x$CH_{2pyrrol.}$), 1.99 (q, 2H, $J = 5.2$ Hz,

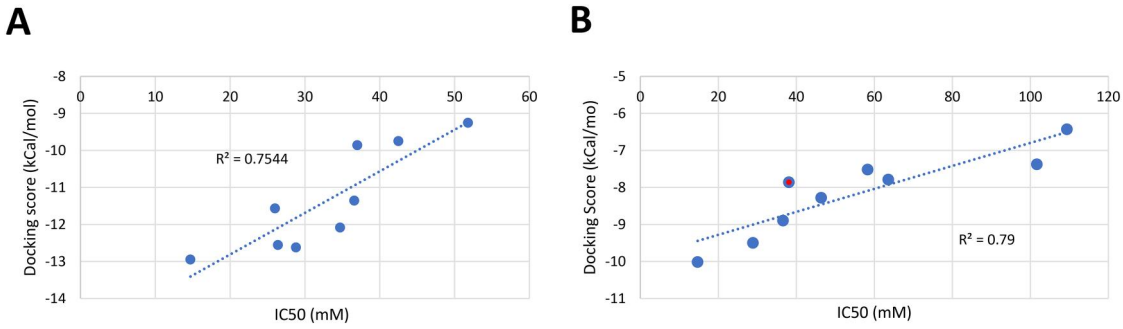

Figure 3. Experimental IC50 vs docking score of 8 compounds against (A) estrogen receptor and (B) aromatase.

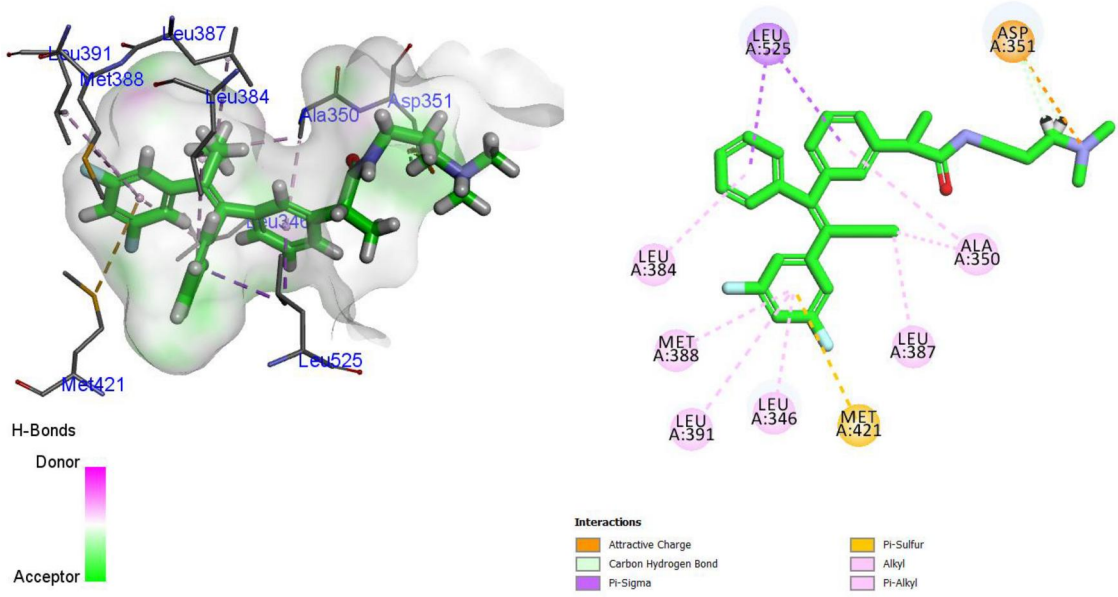

Figure 4. The binding orientation of 12 inside the binding site of estrogen receptor.

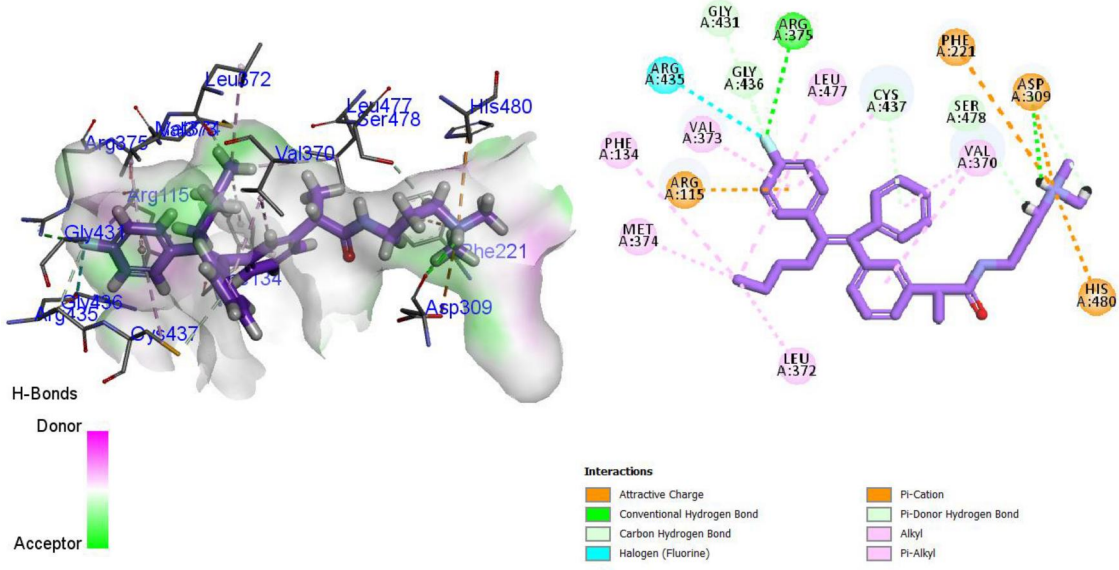

Figure 5. The binding orientation of 10 inside the binding site of aromatase.

CH$_2$CH$_3$), 1.84 (m, 4H, 2xCH$_{2pyrrol.}$), 1.73 (m, 2H, CH$_2$-3′), 1.38 (d, $J = 6.0$ Hz, 3H, C$_2$-Me (R,S isomers). ^{13}C NMR (DMSO-d_6): $\delta = 173.9$ (NHC$_1$=O), 140.0 (C$_{arom.}$-3), 137.4 (C$_{arom.}$-6 + C$_{arom.}$-8), 132,9, 133.3, 132.1, 130.1 128.3, 126.9 (C$_{arom.}$+C$_7$=C$_{12}$), 54.6 ($C^2_{pyrrol.}$+$C^5_{pyrrol.}$), 45.1 (C$_2$-*Me*), 40.0 (NHC-1′+C-4′), (NHC-1′), 29.8 (C-3′), 24.3 ($C^3_{pyrrol.}$+$C^4_{pyrrol.}$), 14.7 (Me). isomers), 1.18 (t, 3H, $J = 5.3$ Hz, CH$_2$CH$_3$). MS (FAB) (*m/z*): $C_{32}H_{38}N_2O$ 466 $[M + H]^+$.

Table 5. Predicted ADME properties of synthesized compounds **9–16** and standard drug tamoxifen.

Compd.	nRB	nHBA	nHBD	TPSA (Å)	BS	GI absorb.	BBB	Pgp	iLOGP	Lipinski
9	11	2	1	32.34	0.55	High	No	Yes	4.7	Yes
10	13	3	1	32.34	0.55	Low	No	Yes	4.62	Yes
11	11	4	2	52.57	0.17	Low	No	Yes	4.73	No,2
12	11	2	1	32.34	0.55	High	No	Yes	4.7	Yes
13	11	2	1	32.34	0.55	High	No	Yes	4.6	Yes
14	13	3	1	32.34	0.17	Low	No	Yes	5.57	No,2
15	11	4	2	52.57	0.17	Low	No	Yes	4.8	No,2
16	11	4	1	32.34	o.17	Low	No	Yes	5.02	No,2
TAM	8	2	0	12.47	0.55	Low	No	Yes	4.64	Yes

2-(3-(2-(4-Fluorophenyl)-1-phenylhex-1-en-1-yl)phenyl)-N-(3-(pyrrolidin-1-yl)propyl)propenamide (14)

From 1-(4-fluorophenyl)pentane-1-one (522 mg). Yield: 358 mg (70%) as a dark brown solid; m.p. 231–233. IR (KBr, cm^{-1}): 3418 (NH), 3180 (Ar*CH*), 2963, 2932 (CH_3), 1649 (C = O_{amide}), 1555 (C = C). ^{1}H NMR (DMSO-d_6): δ = 8.05 (d, 1H, J = 3.1 Hz, 1H, ArH), 8.11–8.01 (m, 3H, ArH), 7.92–7.64 (m, 3H, NH + ArH), 7.61–7.57 (m, 2H, ArH), 7.50–7.41 (m, 1H, ArH), 7.33 (s, 1H, ArH), 3.72 (q, 1H, $J_{H2,Me}$ = 6.0, 1.0 Hz, H-2 (R,S isomers)), 3.23 (m, J = 6.4 Hz, 2H, $NHCH_2$-2′), 2.59 (m, 6H, CH_2-4′+2x$CH_{2pyrrol}$), 1.97 (m, 8H, NMe_2+BuCH_2-1), 1.83 (m, 4H, 2x$CH_{2pyrrol.}$), 1.75 (m, 2H, CH_2-3′), 1.41 (m, 7H, BuCH_2-2 + BuCH_2-3), 1.37 (d, 3H, J = 6.5 Hz, C_2-Me (R,S isomers)), 0.90 (t, 3H, J = 5.3 Hz, BuCH_3). ^{13}C NMR (DMSOd_6): δ = 173.7 (NHC_1=O), 162.7 (d, $J_{C,F}$ = 187 Hz, CF), 143.1 ($C_{arom.}$-8), 137.4 ($C_{arom.}$-3 + $C_{arom.}$-6 + $C_{arom.}$-8), 131.3, 130.0, 129.0, 127.5, 128.7, 127.8, 125.0, 116.5 ($C_{arom.}$+C_7=C_{12}), 54.5 ($C^2{}_{pyrrol.}$+$C^5{}_{pyrrol.}$), 45.4 (C_2-*Me*), 38.0 (NHC-1′+ C-4′), 34.8 (Bu*C-2*), 31.2 ((Bu*C-1*), 29.6 (C-3′), 24.9 ($C^3{}_{pyrrol.}$+$C^4{}_{pyrrol.}$), 22.2 (Bu*C-3*), 14.3 (Bu*Me*+C_2-*Me*). MS (FAB) (*m/z*): $C_{34}H_{41}FN_2O$ 534/536 $[M + Na]^+$.

2-(3-(2-(4-Fluorophenyl)-2-(4-hydroxyphenyl)-1-phenylvinyl)phenyl)-N-(3-(pyrrolidin-1-yl)propyl)propenamide (15)

From (4-Fluorophenyl)(4-hydroxyphenyl)methanone (626 mg). Yield: 395 mg (72%) as a dark brown solid; m.p. 261–262 °C; IR (KBr, cm^{-1}): 3339 (NH), 3063 (Ar*CH*), 2972 (CH_3), 1622 (C = O_{amide}), 1570 (C = C). ^{1}H NMR (DMSO-d_6): δ = 10.51 (s, 1H, OH), 8.23 (m, 1H, NH), 7.95 (s, 2H, ArH), 7.70 (ddd, J = 8.8, 5.5, 2.6 Hz, 4H, ArH), 7.65 (m, 3H, ArH), 7.54 (t, J = 7.6 Hz, 2H, ArH), 7.36 (s, 3H, ArH), 6.91-6.83 (m, 3H, ArH), 3.74 (q, 1H, $J_{H2,Me}$ = 6.0, 1.0 Hz, H-2 (R,S isomers)), 3.35 (m, 2H, NCH_2-2′), 2.57 (m, 6H, CH_2-4′+2x$CH_{2pyrrol.}$), 1.73 (m, 6H, CH_2-3′+2x$CH_{2pyrrol}$), 1.43 (d, J = 6.0 Hz, 3H, C_2-Me (R,S isomers)). ^{13}C NMR (DMSO-d_6): δ = 173.3 (NHC_1=O), 165.8 (d, $J_{C,F}$ = 183 Hz, C-F), 162.6 (C-OH), 143.4 ($C_{arom.}$-6 + $C_{arom.}$-8 + C_7=C_{12}), 135.0 ($C_{arom.}$-3 + $C_{arom.}$-5 + $C_{arom.}$-5′+ $C_{arom.}$-13), 132.0, 130.1, 129.0, 128.8, 128.2, 127.8, 115.8 ($C_{arom.}$), 52.3 ($C^2{}_{pyrrol.}$+$C^5{}_{pyrrol.}$), 40.2 (C_2-Me), 37.9 (NHC-2′+C-4′+Bu*C-2*), 30.4 ((Bu*C-1*), 29.2 (C-3′), 23.0 ($C^3{}_{pyrrol.}$+$C^4{}_{pyrrol.}$+ Bu*C-3*), 14.5 (Bu*Me*+C_2-*Me*). MS (FAB) (*m/z*): $C_{36}H_{37}FN_2O_2$ 547/549 $[M + H]^+$.

2-(3-(2-(3,5-Difluorophenyl)-1-phenylbut-1-en-1-yl)phenyl)-N-(3-(pyrrolidin-1-yl)propyl)propenamide (16)

From 1-(3,5-difluorophenyl)propan-1-one (493 mg). Yield: 291 mg (58%) as a brown-red solid; m.p. 264–265 °C; IR (KBr, cm^{-1}): 3341 (NH), 3061 (ArCH), 2972, 2936 (CH_3), 1657 (C = O_{amide}), 1620 (C = C). ^{1}H NMR (DMSO-d_6): δ = 8.15 (m, 1H, NH), 8.05 (br s., 3H, ArH), 7.72 (m, 2H, ArH), 7.73 (dd, 2H, J = 7.8, 1.7 Hz, ArH), 7.51 (m, 2H, ArH), 6.82 (m, 3H, ArH), 3.72 (q, 1H, J = $J_{H2,Me}$ = 6.0, 1.0 Hz, H-2 (R,S isomers)), 3.40 (m, 2H, $NHCH_2$-2′), 2.55 (m, 6H, CH_2-4′+2x$CH_{2pyrrol}$), 2.23 (q, 2H, J = 5.2 Hz, CH_2CH_3), 1.90 (m, 4H, 2x$CH_{2pyrrol.}$), 1.75 (CH_2-3′), 1.40 (m, 6H, C_2-Me + CH_2CH_3). ^{13}C NMR (DMSO-d_6): δ = 173.8 (NHC_1=O) 162.7 (d, $J_{C,F}$ = 184 Hz, C-F), 143.1 ($C_{arom.}$-8 + $C_{arom.}$-13), 137.4 ($C_{arom.}$-6), 135.3 ($C_{arom.}$-3 + $C_{arom.}$-5 + $C_{arom.}$-5′), 129.0, 128.7, 127.9, 127.2, 125.0, 110.1, 102.8 ($C_{arom.}$+C_7=C_{12}), 52.7 ($C^2{}_{pyrrol.}$+$C^5{}_{pyrrol.}$), 40.5 (C_2-Me), 37.8 (NHC-2′+C-4′), 31.2 (C-3′), 26.2 (CH_2CH_3), 23.7 ($C^3{}_{pyrrol.}$+$C^4{}_{pyrrol.}$), 18.9 (CH_2CH_3), 14.7 (C_2-*Me*). MS (FAB) (*m/z*): $C_{32}H_{36}F_2N_2O$ 524/526 $[M + Na]^+$.

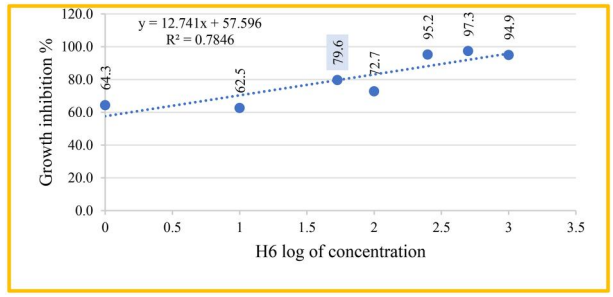

Figure 6. Anticancer activity of compound **14** on MCF7 cells presented by plotting of drug concentration "log" versus GI% values. The colored number resemble the half maximal growth inhibition %.

Biological methods

Microsomal incubation inhibits human aromatase (CYP19)

The aromatase inhibitory activity of tamoxifen derivatives was calculated through the method described by Stresser et al. (2000) and modified by Prachayasittikul et al. (2014). The rate of conversion of the fluorometric substrate 7-methoxy-4-trifluoromethylcoumarin (MFC) to its fluorescence metabolite 7-hydroxytrifluoromethylcoumarin (CYP19) was used to measure the effectiveness of recombinant aromatase (CYP19) (HFC). The experimental procedures were in accordance with the published protocol. All of the incubations were carried out with incubation times and protein conc. that were within the reaction velocity's linear range. Acetonitrile was used to dissolve MFC, the fluorometric substrate, and diluted to a final concentration of 25 mM. The samples were all dissolved in either DMSO or MeOH/DCM (1:1, v/v). The test samples (2 µL) were well stirred with 98 µL of NADPH-Cofactor Mix (16.25 µM NADP+, 825.14 µM $MgCl_2$, 825.14 µM G6P, and 0.4 units/mL G6PD) then warmed at 37 °C for 10 min. A fluorometric substrate, aromatase (CYP 19) human recombinant protein, and 0.1 M KH_2PO_4 buffer (PH 7.4) were used to make an enzyme/substrate mix. Reactions were started by introducing 100 µL of Enz/Submix to volume 200 µL and incubating for 30 min. All reactions were halted by the addition of 75 µL of 0.1 M Tris base soluble in acetonitrile. The quantity of fluorescent output was estimated promptly by monitoring fluorescence response with a BioTek Synergy 2 fluorometric plate reader (Winooski,

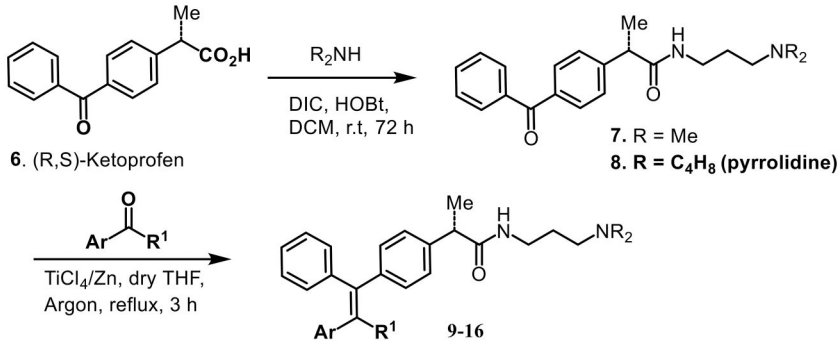

	R	R^1	Ar
9	Me	Et	C_6H_5
10	Me	Bu	4-F-C_6-H_4
11	Me	4-OH-C_6H_4	4-F-C_6-H_4
12	Me	Et	3,5-F_2-C_6-H_3
13	pyrrol.	Et	C_6H_5
14	pyrrol.	Bu	4-F-C_6-H_4
15	pyrrol.	4-OH-C_6H_4	4-F-C_6-H_4
16	pyrrol.	Et	3,5-F_2-C_6-H_3

Scheme 1. Synthesis of new tamoxifen analogues **9–16**.

VT). Excitation–emission wavelengths for MFC metabolite were 409–430 nm. The MFC metabolite standard curve was created using fluorescent metabolites standards. The standard curve's linear regression equation was used to the fluorescent response to quantify the samples. MFC metabolite quantitation limits were 24.7 pmol, with inter- and intracoefficient of variance lower than 10%.

Cell culture and anti-breast cancer assay by MTT method

Human breast cancer cell line MCF-7 and Vero cell lines were used for the test. Cellular viability in the presence and absence of experimental agents was determined using the standard MTT (3-(4,5-Dimethylthiazol-2-yl)-2,5-diphenyltetrazolium bromide) assay (Mosmann, 1983) to assess the anticancer activity of **9–16** against MCF-7. Briefly, cell lines were seeded onto 96 well plates at a density of 1.0 × 105 cells/mL. After incubation for 48 h at 37 °C, and when the confluent monolayer of MCF-7 and Vero cell lines was complete (80–100%), different concentrations (1, 10, 100, 250, 500 and 1000 μg/mL) of microtiter tamoxifen like **9–16**, tamoxifen, plaxitol as a negative control, the maximum concentration of DMSO (0.01%) was employed. To avoid contamination, the microtiter 96 well plates were marched off and transferred to a biohazard safety cabinet after 48 h of incubation at 37 °C in 5% CO_2. All use well media been had been dumped. MCF-7 and Vero cells monolayers were washed with PBS solution to eliminate any residual medications that may interact with MTT reagents. After that, 100 μL of maintenance medium was added to all wells containing drug-treated cells, drug-untreated cells, and blank wells. The MTT reagent (5 mg/mL) was then applied to each well at a volume of 20 μL. After 4 of incubation at 37 °C and 5% CO_2, the formazan particles were generated as a mitochondrial enzymatic process of the unaffected viable MCF-7 and Vero cells. Because the mitochondria organelles in the dead cells were broken, they did not generate formazan particles. The formazan was solubilized by dissolving it in isopropanol with diluted dimethyl sulfoxide DMSO (1:1). An ELISA reader was used to measure the absorbance at 490 nm with a reference wavelength of 630 nm. The mean blank absorption was subtracted from the absorptions of the other samples and controls wells. The data were calculated as a percentage of cell growth inhibition.

Estrogen receptor affinity

The interaction affinity for ER-α and -β were measured by detecting the changes in polarisation values when the investigated drugs displaced the fluorescent oestrogen ligand (ES2). The testing protocols followed the procedure provided by Invitrogen. The ES2 ligand, was given at a concentration of 1800 nM in methanol/water (4:1, v/v). Recombinant human and (ER-α and ER-β) were supplied at concentrations of 734 and 3800 nM in buffers (50 mM BTP, 400 mM KCl, 2 mM DTT, 1 mM EDTA and 10% glycerol). All of the samples evaluated were dissolved in an organic solvent DMSO or mixture of MeOH/DCM (1:1, v/v).

The test samples (1 μL) were thoroughly homogenized with 49 μL of ES2 screening buffers (100 mM K2HPO4, 100 g/mL BGG, and 0.02% NaN3). The ER-α/ES2 complexes were made utilizing the fluorescent estrogen ligand ES2, hRER (ER), and ES2 screening buffer at 9 nM ES2 and 30 nM ER-α.The ER-β/ES2 complexes was created using the fluorescent estrogen ligand ES2, hRER-β (ER-β) and ES2 screening buffer at 9 nM ES2 and 20 nM ER-β concentrations. Reactions were added 50 μL of ER/ES2 mixture to a 100 μL incubating container and incubated for 2 h without illumination. The polarization value was calculated by monitoring the fluorescence response with a BioTek Synergy 2 fluorometric plate

reader (Winooski, VT). The wavelengths of emission spectra for fluorescent polarization were 485–530 nm.

The polarizing values in the presence of the testing competitors were compared to those in the control, which replaced the competitor with a vehicle. The degree of competition was measured as a percentage of the residual polarization in comparison with the control. By fitting all of the values to a one-site competition equation with Graph Pad 5.0, EC50 values were derived as the competitor concentrations that resulted in a half drop in polarization value (GraphPad Software Inc., San Diego, CA).

Docking simulation

First, the 3D structure of designed Tamoxifen derivates was drawn of optimized via ChemDraw. Then the PDBQT format of ligand generated via AutodockTools1.5.6 and also the 3D structures of proteins were prepared and optimized via AutodockTools1.5.6. In next step, Autodock Flexible Residue, (ADFR) was hired to conduct the molecular docking in this work. The advantage of ADFR is take in consideration flexibility of ligands and giving flexibility for receptor side-chains of the binding sites [1]. Before utilizing ADFR, Auto Grid Flexible Residue, (AGFR) is employed to generate the configuration file. Auto Grid maps were obviously built upon the position of reference ligand inside the pocket of the oestrogen receptor (PDB id: 3ERT) and aromatase (PDB id: 3S79). Then the docking results were obtained and analyzed Discovery studio visualizer.

ADME study

Using ChemDraw, the molecular structures of the compounds **9–16** were sketched. After translating these structures to Simplified Molecular Input Line Entry System (SMILES) nomenclature, the prediction process was initiated from website: http://www.swissadme.ch.

Conclusion

A new series of tamoxifen analogues **9–16** have been synthesized from ketoprofen via McMurry reaction as potential aromatase inhibitors. All compounds were evaluated for their aromatase inhibitory and anticancer activity. Compounds **10**, **11** and **12** showed a potent activity against MCF-7 cell lines breast cancer. Where, deeply, compound **12** exhibited potent activity against estrogen receptor (14.7 ± 2.4 nM). Whereas, compound **10** was the most active analogues against aromatase with IC50 of (0.070 nM). The obtained results from docking were correlated with experimental IC50. This study provides useful information to further design new tamoxifen analogues and for further structural modification.

Acknowledgements

We thank University of Kufa of promoting lab equipment's and facilities to accomplish this work.

Disclosure statement

The authors have no financial or personal conflicts that could have influenced their work.

Funding

The author(s) reported there is no funding associated with the work featured in this article.

ORCID

Dunya Al-Duhaidahawi http://orcid.org/0000-0002-1290-6921
Khattab Al-Khafaji http://orcid.org/0000-0002-2165-9256
Najim A. Al-Masoudi http://orcid.org/0000-0001-6811-191X

References

Abdellatif, K. R. A., Belal, A., & Omar, H. A. (2013). Design, synthesis and biological evaluation of novel triaryl (Z)-olefins as tamoxifen analogues. *Bioorganic & Medicinal Chemistry Letters*, *23*(17), 4960–4963. https://doi.org/10.1016/j.bmcl.2013.06.056

Banday, A. H., Saeed, B. A., & Al-Masoudi, N. A. (2021). Synthesis, aromatase inhibitory, antiproliferative and molecular modeling studies of functionally diverse D-ring pregnenolone pyrazoles. *Anti-Cancer Agents in Medicinal Chemistry*, *21*(13), 1671–1679. https://doi.org/10.2174/1871520620999201124213655

Bonneterre, J., Buzdar, A., Nabholtz, J.-M. A., Robertson, J., Thurlimann, B., Euler, V., Sahmoud, T., Webster, A., & Steinberg, M. (2001). Anastrozole is superior to tamoxifen as first-line therapy in hormone receptor positive advanced breast carcinoma: Results of two randomized trials designed for combined analysis. *Cancer*, *92*, 2247–2258.

Bray, F., Ferlay, J., Soerjomataram, I., Siegel, R. L., Torre, L. A., & Jemal, A. (2018). Global cancer statistics 2018:GLOBOCAN estimates of incidence and mortality worldwide for 36 cancers in 185 countries. *CA: A Cancer Journal for Clinicians*, *68*(6), 394–424. https://doi.org/10.3322/caac.21492

Browne, L. J., Gude, C., Rodriguez, R., Steele, E., & Bhatnager, A. (1991). Fadrozole hydrochloride: a potent, selective, nonsteroidal inhibitor of aromatase for the treatment of estrogen-dependent disease. *Journal of Medicinal Chemistry*. *34*, 725–736.

Brueggemeier, R. W., Hackett, J. C., & Diaz-Cruz, E. S. (2005). Aromatase inhibitors in the treatment of breast cancer. *Endocrine Reviews*, *26*(3), 331–345. https://doi.org/10.1210/er.2004-0015

Carlini, P., Frassoldati, A., De Marco, S., Casali, A., Ruggeri, E. M., Nardi, M., Papaldo, P., Fabi, A., Paoloni, F., & Cognetti, F. (2001). Formestane, a steroidal aromatase inhibitor after failure of non-steroidal aromatase inhibitors (anastrozole and letrozole): Is a clinical benefit still achievable? *Annals of Oncology : official Journal of the European Society for Medical Oncology*, *12*(11), 1539–1543. https://doi.org/10.1023/a:1013180214359

Carpenter, C., Zestos, A. G., & Altshuler, R. (2017). (2017) Direct and systemic administration of a CNS-permeant tamoxifen analog reduces amphetamine-induced dopamine release and reinforcing effects. *Neuropsychopharmacology*, *42*, 1940–1949.

Choueiri, T. K., Alemany, C. A., Abou-Jawde, R. M., & Budd, G. T. (2004). Role of aromatase inhibitors in the treatment of breast cancer. *Clinical Therapeutics*, *26*(8), 1199–1214. https://doi.org/10.1016/s0149-2918(04)80017-1

Coombes, R. C., Kilburn, L. S., Snowdon, C. F., Paridaens, R., Coleman, R. E., Jones, S. E., Jassem, J., Van de Velde, C. J., Delozier, T., Alvarez, I., Del Mastro, L., Ortmann, O., Diedrich, K., Coates, A. S., Bajetta, E., Holmberg, S. B., Dodwell, D., Mickiewicz, E., Andersen, J., Lønning, P. E., … & Intergroup Exemestane Study (2007). Survival and safety of exemestane versus tamoxifen after 2-3 years' tamoxifen treatment (Intergroup Exemestane Study): a randomised controlled trial. *Lancet (London, England)*, *369*(9561), 559–570. https://doi.org/10.1016/S0140-6736(07)60200-1

Cronin-Fenton, D. P., Damkier, P., & Lash, T. L. (2014). Metabolism and transport of tamoxifen in relation to its effectiveness: new perspectives on an ongoing controversy. *Future Oncology*, *10*, 107–122.

Cuzick, J., Sestak, I., Cawthorn, S., Hamed, H., Holli, K., Howell, A., Forbes, J. F., & IBIS-I Investigators (2015). Tamoxifen for prevention of breast cancer: extended long-term follow-up of the IBIS-I breast cancer prevention trial. *The Lancet. Oncology*, *16*(1), 67–75. https://doi.org/10.1016/S1470-2045(14)71171-4

Davies, C., Pan, H., Godwin, J., Gray, R., Arriagada, R., Riana, V., Abraham, M., Medeiros Alencar, V. H., Badran, A., Bonfill, X., Bradbury, J., Clarke, M., Collins, R., Davis, S. R., Delmestri, A., Forbes, J. F., Haddad, P., Hou, M.-F., Inbar, M. … Peto, R. (2013). Long-term effects of continuing adjuvant tamoxifen to 10 years versus stopping at 5 years after diagnosis of estrogen receptor-positive breast cancer: ATLAS, a randomised trial. *Lancet*, *381*, 805–816.

Diana, A., Michielin, O., & Zoete, V. (2017). SwissADME: A free web tool to evaluate pharmacokinetics, drug-likeness and medicinal chemistry friendliness of small molecules. *Scientific Reports*, *7*(1). https://doi.org/10.1038/srep42717

Double, J., Maitland, D., & Popa, I. (2001). Tamoxifen and analogues thereof. (Patent No. 6172263). In *US Patent* (No. 6172263).

Elghazawy, N. H., Engel, M., Hartmann, R. W., Hamed, M. M., Ahmed, N. S., & Abadi, A. H. (2016). Design and synthesis of novel flexible ester-containing analogs of tamoxifen and their evaluation as anticancer agents. *Future Medicinal Chemistry*, *8*(3), 249–256. https://doi.org/10.4155/fmc.15.181

Ellis, M. J., Llombart-Cussac, A., Feltl, D., Dewar, J. A., Jasiówka, M., Hewson, N., Rukazenkov, Y., & Robertson, J. F. R. (2015). Fulvestrant. 500 mg versus anastrozole 1 mg for the first-line treatment of advanced breast cancer: Overall survival analysis from the phase II FIRST study. *Journal of Clinical Oncology*, *33*(32), 3781–3787. https://doi.org/10.1200/JCO.2015.61.5831

Ferlay, J., Soerjomataram, I., Dikshit, R., Eser, S., Mathers, C., Rebelo, M., Parkin, D. M., Forman, D., & Bray, F. (2015). Cancer incidence and mortality worldwide: Sources, methods and major patterns in GLOBOCAN 2012. *International Journal of Cancer*, *136*(5), E359–86. https://doi.org/10.1002/ijc.29210

Fisher, B., Costantino, J. P., Wickerham, D. L., Cecchini, R. S., Cronin, W. M., Robidoux, A., Bevers, T. B., Kavanah, M. T., Atkins, J. N., Margolese, R. G., Runowicz, C. D., James, J. M., Ford, L. G., & Wolmark, N. (2005). Tamoxifen for the prevention of breast cancer: Current status of the national surgical adjuvant breast and bowel project P-1 study. *Journal of the National Cancer Institute*, *97*(22), 1652–1662. https://doi.org/10.1093/jnci/dji372

Gaillard, S., & Stearns, V. (2011). Aromatase inhibitor-associated bone and musculoskeletal effects: New evidence defining etiology and strategies for management. *Breast Cancer Research*, *BCR*, *13*(2), 205. https://doi.org/10.1186/bcr2818

Hyder, T., Marino, C. C., Ahmad, S., Nasrazadani, A., & Brufsky, A. M. (2021). Aromatase inhibitor-associated musculoskeletal syndrome: Understanding mechanisms and management. *Frontiers in Endocrinology*, *12*, 713700. https://doi.org/10.3389/fendo.2021.713700

Jordan, V. C., & Brodie, A. M. (2007). Development and evolution of therapies targeted to the estrogen receptor for the treatment and prevention of breast cancer. *Steroids*, *72*(1), 7–25. https://doi.org/10.1016/j.steroids.2006.10.009

Lu, W. J., Xu, C., Pei, Z., Mayhoub, A. S., Cushman, M., & Flockhartet, D. A. (2012). The tamoxifen metabolite norendoxifen is a potent and selective inhibitor of aromatase (CYP19) and a potential lead compound for novel therapeutic agents. *Breast Cancer Research and Treatment*, *133*, 99–109.

Lv, W., Liu, J., Lu, D., Flockhart, D. A., & Cushman, M. (2013). Synthesis of mixed (*E,Z*)-, (*E*)-, and (*Z*)- norendoxifen with dual aromatase inhibitory and estrogen receptor modulatory activities. *Journal of Medicinal Chemistry*, *56*, 4611–4618.

Mosmann, T. (1983). Rapid colorimetric assay for cellular growth and survival: Application to proliferation and cytotoxicity assays. *Journal of Immunological Methods*, *65*(1–2), 55–63. https://doi.org/10.1016/0022-1759(83)90303-4

Ohta, K., Kaise, A., Taguchi, F., Aoto, S., Ogawa, T., & Endo, Y. (2019). Design and synthesis of novel breast cancer therapeutic drug candidates based upon the hydrophobic feedback approach of antiestrogens. *Molecules*, *24*, 3966–3978.

Olier-Reuchet, C., Aitken, D. J., & Husson, H.-P. (1998). Synthesis of C-ring aza-analogues of tamoxifen. *Heterocyclic Communications*. *4*, 59–62.

Prachayasittikul, V., R. Pingaew, R., C. Nantasenamat, C., S. Prachayasittikul, S., S. Ruchirawat, S., & V. Prachayasittikul, V. (2014). Investigation of aromatase inhibitory activity of metal complexes of 8-hydroxyquinolineand uracil derivatives. *Drug Design, Development and Therapy*, *8*, 1089–1096.

Sharma, D., Kumar, S., & Narasimhan, B. (2018). Estrogen alpha receptor antagonists for the treatment of breast cancer: A review. *Chemistry Central Journal*, *12*(1), 107–139. https://doi.org/10.1186/s13065-018-0472-8

Srikanth, N., Tan, C.-H., Ng, S.-C., Loh, T.-P., Koh, L.-L., & Sim, K.-Y. (1997). Synthesis of heterocyclic analogues of tamoxifen as potential antiestrogens. *Journal of Chemical Research, Synopses*, *8*, 274–275. https://doi.org/10.1039/a701410d

Stresser, D. M., Turner, S. D., McNamara, J., Stocker, P., Miller, V. P., Crespi, C. L., & Patten, C. J. (2000). A high throughput screen to identify inhibitors of aromatase (CYP19. *Analytical Biochemistry*, *284*(2), 427–430. https://doi.org/10.1006/abio.2000.4729

Willker, W., Leibfritz, D., Kerssebaum, R., & Bermel, W. (1993). Gradient selection in inverse heteronuclear correlation spectroscopy. *Magnetic Resonance in Chemistry MRC*, *31*(3), 287–292. https://doi.org/10.1002/mrc.1260310315